Conductance Mutations of the Nicotinic Acetylcholine Receptor Do Not Act by a Simple Electrostatic Mechanism

Paul Kienker,* Gordon Tomaselli, Mark Jurman,‡ and Gary Yellen‡
Howard Hughes Medical Institute and the Departments of Neuroscience, Biophysics, and Medicine, The Johns Hopkins University School of Medicine, Baltimore, Maryland 21205 USA

ABSTRACT Fixed negative charges in many cation channels raise the single-channel conductance, apparently by an electrostatic mechanism: their effects are accentuated in solutions of low ionic strength and attenuated at high ionic strength. The charges of specific amino acids near the ends of the proposed pore-lining M2 segment of the nicotinic acetylcholine receptor, termed the extracellular and cytoplasmic rings, have recently been shown to influence the single-channel K^+ conductance (Imoto, K., C. Busch, B. Sakmann, M. Mishina, T. Konno, J. Nakai, H. Bujo, Y. Mori, K. Fukuda and S. Numa. 1988. *Nature* 335:645–648). We examined whether these charges might act by a direct electrostatic effect on the energy of ions in the pore, rather than indirectly by inducing a structural change. To this end, we measured the conductances of charge mutants over a range of K^+ concentrations (ionic strengths). As expected, we found that negative charge mutations raise the conductance, and positive charge mutations lower it. The effects of cytoplasmic-ring mutations are accentuated at low ionic strength, but they are not completely attenuated at high ionic strength. The effects of extracellular-ring mutations are independent of ionic strength. These results are inconsistent with the simplest electrostatic model. We suggest a modified model that qualitatively accounts for the data.

INTRODUCTION

The unitary conductances of many ion channels are affected by fixed charges (Green and Andersen, 1991). This has been demonstrated by several approaches: screening of charge with high ionic strength or divalent cations, changing pH, changing lipid charge in reconstitution experiments, and changing the fixed charge on the channel by chemical modification or site-directed mutagenesis. In most cases a fixed negative charge increases the cation conductance, whether the charge resides on the channel (Apell et al., 1977; Sigworth and Spalding, 1980; Adams, 1983; Reinhardt et al., 1986; Worley et al., 1986; MacKinnon et al., 1989; Roeske et al., 1989) or on the membrane lipids (Apell et al., 1979; Bell and Miller, 1984; Moczydlowski et al., 1985; Coronado and Affolter, 1986). An exception is the hemocyanin model channel, for which negative lipid charge decreases the cation current (Cecchi et al., 1981). For almost all cases studied, the effect of fixed charges on conductance is more pronounced at low ionic strength and is attenuated at high ionic strength (Apell et al., 1977, 1979; Bell and Miller, 1984; Moczydlowski et al., 1985; Coronado and Affolter, 1986; MacKinnon et al., 1989; Roeske et al., 1989), suggesting a through-space electrostatic effect. In one proposed mechanism, negative charges raise conductance by raising the local concentration of permeant cations in the mouth of the pore.

The location of the modified charges in the primary amino-acid sequence is unknown in the examples cited above, except in the studies of carboxyl-terminal charged analogues of the model channel gramicidin A. The first identification of specific residues whose charge affected the conductance of an ion-channel protein came from mutagenesis of the nicotinic acetylcholine receptor (AChR) (Imoto et al., 1988). It was suggested that AChR charge mutations might act by an electrostatic mechanism (Imoto et al., 1986; Konno et al., 1991), consistent with other evidence that a negative local potential affects AChR conductance (Lewis and Stevens, 1979; Dani and Eisenman, 1987). In the only study of the ionic-strength dependence of a charge-modified AChR, it was found that neutralization of exposed carboxyl groups by extracellularly applied trimethyloxonium reduced AChR single-channel conductance equally at 15 and 177 mM extracellular ionic strength (Pappone and Barchfeld, 1990). This surprising independence from ionic strength appears to rule out a simple electrostatic mechanism.

We have measured the ionic-strength dependence of AChR single-channel conductance changes caused by site-directed charge mutations, and compared these data with the predictions of an electrostatic model. Our goals were first, to test whether the effects of the mutations identified by Imoto et al. (1988) were more pronounced at low ionic strength and attenuated at high ionic strength; and second, to look for effects of a mutation more distant from the pore by using solutions of low ionic strength. In addition, we wished to determine whether any electrostatic mechanism could explain ionic-strength-independent conductance changes.

Received for publication 17 August 1992 and in final form 8 November 1993.
Address reprint requests to Gary Yellen.

* Current address: Du Pont Merck Pharmaceutical Company, Experimental Station, Wilmington, DE 19880-0328.

‡ Current address: Department of Neurobiology, Harvard Medical School, and the Massachusetts General Hospital, Boston, MA 02114.

0006-3495/94/02/325/10 $2.00

THEORY

We relate AChR conductance to ion concentration and surface charge using a combination of a rate-theory permeation model and a Gouy-Chapman surface-potential model; this theoretical framework has been used previously for the AChR (Lewis and Stevens, 1979; Villarroel and Sakmann, 1992) and other ion channels (Green and Andersen, 1991). Rather than attempting to specify the parameters of a detailed rate-theory model, we limit our analysis to general features of this class of models. Single-ion occupancy rate-theory permeation models predict that the single-channel chord conductance g (current/voltage) should depend on the permeant-ion concentration C according to the formula

$$g = g_{max}/(1 + K_m/C), \quad (1)$$

where g_{max} is the maximum conductance and K_m is the ion concentration at which the conductance is half-maximal (Läuger, 1973). Both g_{max} and K_m are functions of the transmembrane voltage and the energy barriers to ion permeation, so different values may apply for inward and outward conductances. Equation 1 does not fit the AChR conductance-concentration relation (Dani and Eisenman, 1987). A common solution is to postulate that the AChR carries a negative surface potential, which raises the local permeant-cation concentration C_0 at the pore mouth relative to its bulk concentration, thereby raising the ion entry rate into the channel. Then the concentration C in Eq. 1 is replaced by

$$C_0 = C \exp(-z_K \phi_0 F/RT), \quad (2)$$

where z_K is the permeant-ion valence and ϕ_0 is the local potential at the pore mouth; F, R, and T are the Faraday constant, gas constant, and absolute temperature. Combining Eqs. 1 and 2 gives the formula

$$g = g_{max}/[1 + (K_m/C)\exp(z_K \phi_0 F/RT)]. \quad (3)$$

According to this model, changes in channel charge can alter an ion's apparent affinity for the channel, but do not affect the maximum conductance.

The potential ϕ_0 depends on the geometry of the fixed charges, channel, and membrane, and on the ionic strength I of the electrolyte. The Gouy-Chapman double-layer theory treats a simplified geometry, with a uniform fixed surface-charge density σ on an infinite planar membrane, bathed on one side by electrolyte; the surface potential ϕ_0 in a 1:1 electrolyte is given by

$$\phi_0 = (2RT/F)\sinh^{-1}[\sigma(8\varepsilon\varepsilon_0 RTI)^{-0.5}] \quad (4)$$

(McLaughlin, 1989). Here ε is the dielectric constant of the electrolyte and ε_0 is the permittivity of free space. In a 1:1 electrolyte I equals the bulk salt concentration C. To describe the effect of a charge mutation on the surface-charge density, we divide the change in charge valence Δz by an effective area A:

$$\sigma = \sigma_{native} + e\Delta z/A, \quad (5)$$

where e is the elementary charge.

As the ionic strength decreases, the magnitude of the surface potential increases, so a charge mutation should have a greater effect on the conductance. As the ionic strength increases, the surface potential becomes smaller, so a charge mutation should have little effect on the conductance. The surface-charge densities σ_{cyt} in the cytoplasmic mouth and σ_{ext} in the extracellular mouth of the pore may differ; in this model σ_{cyt} affects the outward conductance and σ_{ext} affects the inward conductance.

METHODS

Mutagenesis and RNA transcription

The murine (BC3H-1) AChR α, β, γ, and δ-subunit DNAs were generously provided by Dr. J. Boulter of the Salk Institute. Mutations were made using dut⁻ and ung⁻ selection, cDNAs were sequenced and in vitro RNA transcription was performed as previously described, with minor modifications (Tomaselli et al., 1991). The cytoplasmic-ring mutations are α-D238K and δ-D252K, where α-D238K means D at residue 238 of the α subunit is replaced by K (Fig. 1). The extracellular-ring mutations are α-E262Q, γ-K271Q, δ-K276Q, δ-K276E, and combinations of these. The mutation in the proposed M2-M3 loop is δ-R277E.

Preparation of oocytes

Xenopus laevis oocytes were prepared and injected with AChR subunit RNAs mixed in a ratio of 2α:1β:1γ:1δ as described (Tomaselli et al., 1991). Oocytes were kept at 18°C

```
          238                 241                                                 262
alpha   Thr Asp Ser Gly --- Glu Lys Met Thr Leu Ser Ile Ser Val Leu Leu Ser Leu Thr Val Phe Leu Leu Val Ile Val Glu Leu Ile
          272                 275                                                 296
beta    Pro Asp Ala Gly --- Glu Lys Met Gly Leu Ser Ile Phe Ala Leu Leu Thr Leu Thr Val Phe Leu Leu Leu Leu Ala Asp Lys Val
          246                 250                                                 271
gamma   Ala Lys Ala Gly Gly Gln Lys Cys Thr Val Ala Thr Asn Val Leu Leu Ala Gln Thr Val Phe Leu Phe Leu Val Ala Lys Lys Val
          252                 255                                                 276 277
delta   Gly Asp Cys Gly --- Glu Lys Thr Ser Val Ala Ile Ser Val Leu Leu Ala Gln Ser Val Phe Leu Leu Leu Ile Ser Lys Arg Leu
          CR                  IR                                                  ER

     M1  ]                  [---------------------- M2 ----------------------]
```

FIGURE 1 Aligned mouse AChR subunit amino-acid sequences surrounding the proposed M2 segment. Mutated residues are underlined. Residues corresponding to the cytoplasmic, intermediate, and extracellular rings identified in the *Torpedo* AChR by Imoto et al. (1988) are denoted by CR, IR, and ER, respectively. References for sequences: α, Boulter et al. (1985); β, Buonanno et al. (1986); γ, Yu et al. (1986); δ, LaPolla et al. (1984).

for 1–10 days before patch recording. No systematic dependence of single-channel conductance on oocyte age was detected.

Electrophysiology

Selected oocytes were screened for acetylcholine (ACh)-induced current by two-microelectrode voltage clamp and oocytes were prepared for patch-clamp recording as described (Tomaselli et al., 1991). Excised outside-out patches were obtained in symmetric pipette and bath solutions. The K^+ recording solutions contained a variable amount of KCl (J. T. Baker, Phillipsburg, NJ) with 4 mM 4-(2-hydroxyethyl)-1-piperazineethanesulfonic acid (HEPES), 0.2 mM EDTA, sorbitol to raise the osmolarity to 211 mM (Sigma Chemical Co., St. Louis, MO), and KOH (J. T. Baker) to pH 7.5. Solutions are named by the total cation concentration. For some experiments (see Tables 3 and 4) EGTA was used in place of EDTA; there was no apparent effect on conductance. For other experiments (noted in the text) 0.1 or 1 mM $MgCl_2$ was added to EGTA-containing solutions. For the 500 mM K^+ experiments, patches were formed with 500 mM K^+ in the pipette solution and 200 mM K^+ in the bath solution; after patch excision the bath was perfused with at least 5 volumes of 500 mM K^+ before recording. A salt bridge containing 500 mM K^+ and 1% agarose (BRL, Gaithersburg, MD) was used with the bath electrode in those experiments. The dimethylammonium (DMA^+) recording solution was made from 200 mM dimethylamine (from 40% aqueous solution, Aldrich Chemical Co., Milwaukee, WI), 10 mM HEPES, 1 mM EDTA, and HCl (J. T. Baker) to pH 7.5. Patches were inserted into the perfusion inlet and alternately perfused with control and ACh-containing solutions (0.1–5 μM in K^+, 5–20 μM in DMA^+), using a T-valve to switch between the two. Channel activity was correlated with ACh application. In the DMA^+ solution there was a low level of activity without ACh application, as previously reported for other alkyl amines (Sanchez et al., 1986); these channels had a current-voltage relation identical to those activated by ACh. Currents were recorded with a List EPC-7 (List-electronic, Darmstadt, Germany) or an Axopatch 1-D (Axon Instruments, Foster City, CA) patch-clamp amplifier, lowpass filtered at 1–5 kHz (8-pole Bessel, −3 dB; Frequency Devices, Haverhill, MA), digitized at 10–33 kHz on a Cheshire Data interface (Indec, Sunnyvale, CA), and stored on computer disk. The single-channel current-voltage relations were obtained using rampwise or steady-state voltage changes, controlled through the Indec interface. All recordings were done at room temperature, 20–25°C.

Data analysis

Unitary-current amplitudes were fit by eye using a computer-analysis program. Only well-resolved openings were measured (Fig. 2). Subconductance levels were excluded; multiple conductance levels were most commonly observed at voltages more negative than −100 mV. The inward (−100 to −10 mV) and outward (10 to 100 mV) segments of the current-voltage relation were fit separately by straight lines with a least-squares algorithm; the slope is reported as the conductance. Typically 100 to 1000 channel events contributed to each conductance determination. We apply the theoretical chord-conductance equations directly to the slope-conductance data. Theoretical functions were fit to the conductance data using the programs KaleidaGraph (Synergy Software, Reading, PA), and MLAB (Civilized Software, Bethesda, MD). In all but a few cases each patch came from a different oocyte (see Tables 1 and 5).

We assume throughout our analysis that the amino-acid side chains have the charge valence expected at neutral pH: Asp and Glu, −1; Gln, 0; Arg and Lys, 1.

RESULTS

Effects of extracellular-ring mutations at constant ionic strength

We first attempted to replicate in our system the result Imoto et al. (1988) found for the *Torpedo* AChR: that increasing the net positive charge of the extracellular ring decreases the inward conductance in 100 mM K^+. Single-channel current traces in 100 mM K^+, at −100 mV, for native AChR and the mutant α-E262Q are shown in Fig. 2; as expected, the positive charge mutation lowers the current amplitude. From the

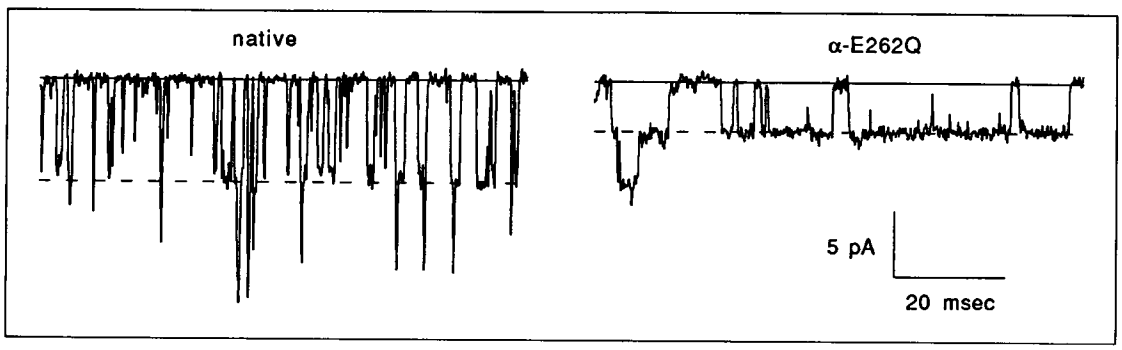

FIGURE 2 Single-channel current versus time at −100 mV holding potential, in 100 mM K^+. The solid line marks the baseline current level, while the dashed line marks the open-channel current level. Left, native AChR; right, extracellular-ring mutant α-E262Q.

TABLE 1 Inward and outward conductances (pS) of native AChR and extracellular-ring mutants in 100 mM K^+ or 200 mM DMA^+

$\alpha\beta\gamma\delta$	z_{ER}	g_{in} (K^+)	g_{out} (K^+)	g_{in} (DMA^+)
EDQE	−4	107 ± 2 (7)	95 ± 1 (2)	49.5 ± 0.5 (2)*
EDQQ	−3	103 ± 1 (3)	87 ± 7 (2)	ND‡
EDKE	−3	102 ± 1 (8)	91 ± 2 (5)	45 ± 2 (2)
EDKQ	−2	95 ± 2 (3)	84 ± 2 (3)	ND
EDQK	−2	90 ± 1 (5)	81 ± 3 (3)	50 ± 2 (2)
QDKE	−1	89.0 ± 0.5 (2)	82.5 ± 0.5 (2)	ND
EDKK	−1	79.5 ± 0.9 (4)	76 ± 2 (4)	40.8 ± 0.5 (4)
QDKQ	0	74 ± 2 (2)	ND	ND
QDQK	0	65 ± 5 (2)	ND	ND
QDKK	1	45 ± 0.5 (6)	52.5 ± 0.5 (2)	ND

$\alpha\beta\gamma\delta$: extracellular-ring amino acids in single-letter code: D, Asp; E, Glu; K, Lys; Q, Gln; R, Arg. z_{ER}: net extracellular-ring valence. g_{in} and g_{out}: inward and outward single-channel conductances, presented as mean and standard error, with the number of patches in parentheses.

* Both patches came from a single oocyte.

‡ ND, not determined.

full current-voltage relations we can see that this mutation decreases both inward and outward conductance, while the negative charge mutation δ-K276E increases the conductance (Fig. 3 *A*). All the mutants we have studied either raise or lower both the inward and outward conductances together. Using mutants with net extracellular-ring charge from −4 to 1 (native mouse AChR = −1; *Torpedo* = −3), we reproduced the earlier results (Fig. 4, Table 1). The data are well fit by the simple electrostatic model of Eqs. 3–5 (Table 2). The outward conductance has a similar dependence on the extracellular-ring charge (Table 1); these data are also well fit by the simple electrostatic model (Table 2).

The mutation α-E262Q increases the open-channel lifetime substantially (Fig. 2), as does the mutation δ-K276E (data not shown). Because mutations of opposite polarity have similar effects, the change in open lifetime cannot be due to a simple electrostatic mechanism.

To test whether the effects of the mutations depend on the size of the permeant ion, we also measured inward conductance in 200 mM DMA^+ (Fig. 4 and Table 1). These data can be fit by the same parameters as for K^+, except with g_{max} = 55 pS.

Ionic-strength dependence of extracellular-ring mutations

We next measured the ionic-strength dependence of extracellular-ring mutations. The currents of the native AChR and the mutants α-E262Q and δ-K276E are smaller in 15 mM K^+ than in 100 mM K^+, but all the currents decrease by about the same proportion (Fig. 3 *B*). The inward conductance (Fig. 5 *A* and Table 3) and the mutant/native inward-conductance ratio (Fig. 5 *B*) are plotted against [K^+]; the conductance ratios show no clear ionic-strength dependence between 15 and 500 mM K^+. The simple electrostatic model of Eqs. 3 and 4 requires that mutations do not change the maximum conductance g_{max}. This model does not fit the native and mutant data well; the best fit under this constraint is shown in Fig. 5 (*dashed lines*). Of course the fits can be improved if the mutations are allowed to change g_{max}.

The increase in outward conductance produced by the mutation δ-K276E also persists at high [K^+]: the outward-conductance ratio is 1.20 in 100 mM K^+ and 1.18 in 500 mM K^+ (Table 4).

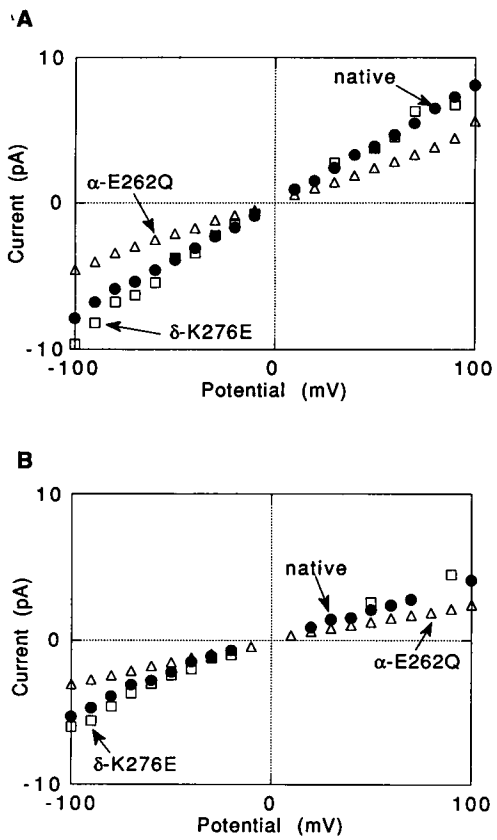

FIGURE 3 Single-channel current-voltage relations for native AChR (*circles*) and the extracellular-ring mutants α-E262Q (*triangles*) and δ-K276E (*squares*). (*A*) 100 mM K^+; (*B*) 15 mM K^+.

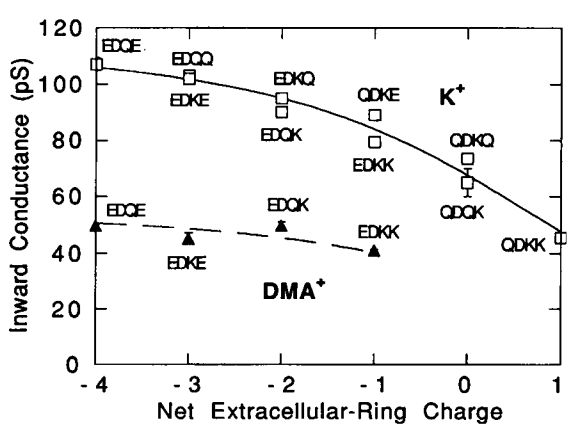

FIGURE 4 Single-channel AChR inward conductance in 100 mM K^+ (*squares*) and 200 mM DMA^+ (*triangles*), plotted against net extracellular-ring charge. The four-letter code indicates the extracellular-ring amino acids in the α, β, γ, and δ subunits, respectively. The curves represent the best fits of the simple electrostatic model of Eqs. 3–5.

TABLE 2 Best-fit parameters of simple electrostatic model

Parameter	Inward conduction		Outward conduction	
	$g(\Delta z)$	$g(K)$	$g(\Delta z)$	$g(K)$
g_{max} (pS)	116	135	99	93
σ_{native} (e/nm^2)	−0.16	−0.16	−0.05	−0.05
A (nm^2)	12	NA*	16	NA
K_m (mM)	NA	151 (Δz = −2)	45 (Δz = 0)	38 (Δz = 0)
	130 (Δz = 0)	297 (Δz = 0)	NA	61 (Δz = 2)
	NA	914 (Δz = 2)	NA	144 (Δz = 4)

$g(\Delta z)$: Fit of conductance-charge data. σ_{native} is taken from the $g(K)$ fit, as it is impractical to determine K_m and σ_{native} independently at constant ionic strength. $g(K)$: Fit of conductance-concentration data. If the mutations are allowed to change σ, but σ is required to change in the same direction as the polarity of the mutation, the fit produces equal σ values. Parameters are from Eqs. 3–5. The native AChR and each mutant (identified by Δz) has its own K_m in the conductance-concentration fit.

* NA, not applicable.

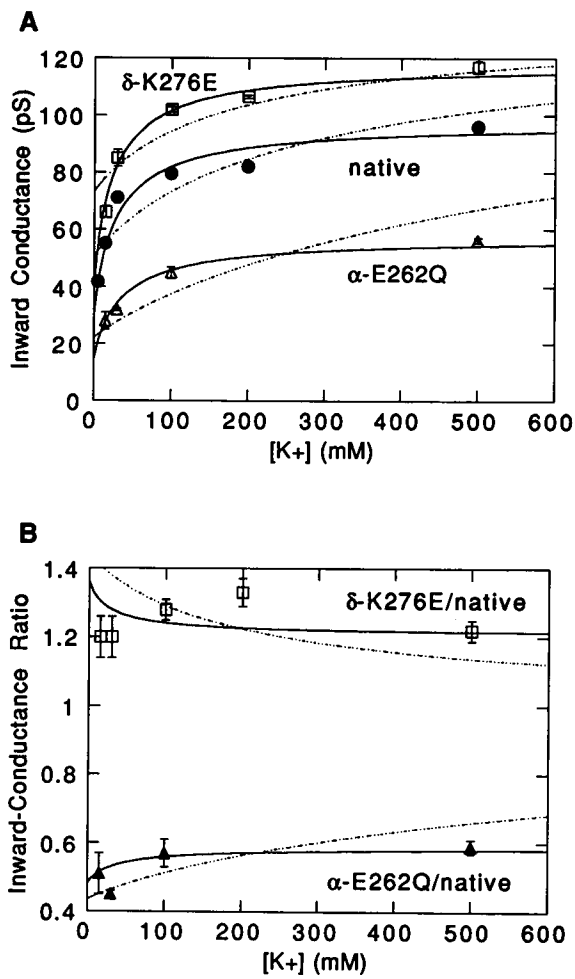

FIGURE 5 (*A*) Inward conductance of native AChR (*circles*) and extracellular-ring mutants δ-K276E (*squares*) and α-E262Q (*triangles*), plotted against [K$^+$]. (*B*) Mutant/native inward-conductance ratio versus [K$^+$]. The data in both figures are fit using the simple electrostatic model of Eqs. 3 and 4 (*dashed lines*) and the concentration-saturation model of Eq. 8 (*solid lines*).

Ionic-strength dependence of cytoplasmic-ring mutations

We then studied the ionic-strength dependence of cytoplasmic-ring mutations. The outward conductance (Fig. 6 *A* and Table 4) and the mutant/native outward-conductance ratio (Fig. 6 *B*) for the native AChR and the mutations δ-D252K and α-D238K are plotted against [K$^+$]. In contrast to the extracellular-ring results, both cytoplasmic-ring mutations reduce the conductance more at lower ionic strength, as expected for an electrostatic mechanism. Like the extracellular-ring mutants, however, their effects are not completely attenuated at high ionic strength. Thus the simple electrostatic model cannot fit all the curves well; the best fit using a common g_{max} (Table 2) is shown in Fig. 6 (*dashed lines*).

Effect of magnesium on an extracellular-ring mutation

We investigated whether Mg^{2+} reduces the effect of an extracellular-ring mutation, where 500 mM K$^+$ had no effect. The extracellular-ring mutation α-E262K has been shown to diminish Mg^{2+} block of inward conductance in the *Torpedo* AChR (Imoto et al., 1988). We find that as [Mg^{2+}] increases, the δ-K276E/native conductance ratio decreases toward 1 (Table 5). The effect of increasing [Mg^{2+}] is qualitatively what we had expected from increasing the ionic strength. Although 1 mM Mg^{2+} contributes much less to the ionic strength than 500 mM K$^+$, the ionic strength may underestimate the screening ability of divalent ions at a highly charged membrane surface, due to the nonlinearity of the Gouy-Chapman potential and specific ion binding to fixed charges (McLaughlin et al., 1971).

A more distant mutation

The double-layer theory predicts that the potential produced by a charge extends further at lower ionic strength. We studied a mutation in the proposed M2–M3 loop which had been reported not to affect the conductance in 100 mM K$^+$ (Imoto et al., 1988) to see if it became effective at lower ionic strength. The mutation δ-R277E is just beyond the extracellular ring in the primary sequence. This mutation causes a slight increase in the inward conductance, but there is no clear ionic-strength dependence between 15 and 500 mM K$^+$

TABLE 3 Inward conductances (pS) of native AChR and mutants at various K^+ concentrations

Channel	Group	5.4 mM	15 mM	30 mM	100 mM	200 mM	500 mM
Native		41.7 ± 0.7(3)*	55 ± 1 (4)	71 ± 1 (4)	79.5 ± 0.9 (4)	82 ± 1 (10)*	96 ± 1 (2)
αD238K	CR	ND	ND	ND	65.5 ± 0.5 (2)	72 ± 2 (2)	ND
δD252K	CR	ND	55 ± 2 (4)	59 ± 4 (2)	77 ± 2 (3)	82 ± 3 (2)	92 ± 2 (2)
αE262Q	ER	ND	28 ± 3 (3)	32.0 ± 0.5 (4)	45.0 ± 0.5 (6)	ND	56.3 ± 0.9 (3)
δK276E	ER	ND	66 ± 2 (5)*	85 ± 3 (2)*	102 ± 1 (8)	106.5 ± 0.5 (2)*	117 ± 2 (2)
δR277E	M2–M3	ND	61.7 ± 0.8 (6)*	70 ± 2 (2)	78 ± 2 (6)*	88 ± 3 (4)*	106 (1)

CR, cytoplasmic ring; ER, extracellular ring; M2–M3, M2–M3 loop. Conductances are presented as mean and standard error, with the number of patches in parentheses. ND, not determined. Averages which include one or more experiments using EGTA-containing solutions are marked with an asterisk (*).

TABLE 4 Outward conductances (pS) of native AChR and mutants at various K^+ concentrations

Channel	Group	15 mM	30 mM	100 mM	200 mM	500 mM
Native		48.0 ± 0.5 (2)	54.7 ± 0.9 (3)	76 ± 2 (4)	78 ± 2 (4)*	91.7 ± 0.5 (3)
αD238K	CR	22 ± 1 (2)	30 ± 1 (2)	52 ± 1 (2)	56 ± 2 (2)	66 ± 3 (2)
δD252K	CR	31.5 ± 0.5 (2)	46 ± 2 (3)	70 ± 3 (3)	76.7 ± 0.5 (3)	84 ± 2 (3)
δK276E	ER	ND	ND	91 ± 2 (5)	ND	108 ± 2 (2)
δR277E	M2–M3	49 ± 2 (2)	ND	ND	82 ± 5 (3)*	ND

CR, cytoplasmic ring; ER, extracellular ring; M2–M3, M2–M3 loop. Conductances are presented as mean and standard error, with number of patches in parentheses. ND, not determined. Averages which include one or more experiments using EGTA-containing solutions are marked with an asterisk (*).

TABLE 5 Inward conductances (pS) of native and mutant AChR in K^+ solutions with added Mg^{2+}

$[K^+]$	$[Mg^{2+}]$	Native	δK276E
mM	mM		
5.4	0.1	10 ± 1 (2)	ND
15	0.1	28 ± 2 (2)	ND
50	0.1	58 ± 2 (4)	60.0 ± 0.5 (2)
100	0.1	68 ± 3 (2)	83 ± 2 (2)
200	0.1	78 ± 1 (4)	97 ± 3 (2)
30	1	22 ± 1 (2)	ND
50	1	34 ± 3 (3)	30 ± 2 (2)
100	1	49 ± 1 (3)	55.5 ± 0.5 (2)*
200	1	ND	76 ± 1 (2)

Conductances are presented as mean and standard error, with number of patches in parentheses. ND, not determined.
* Both patches came from a single oocyte.

(Table 3). This could be related to the ionic-strength independence of the extracellular-ring mutants.

DISCUSSION

We have confirmed that the AChR K^+ conductance decreases with increasing net positive charge of the extracellular and cytoplasmic-ring residues identified by Imoto et al. (1988). The charge dependence we observe in the mouse AChR conductance matches well the earlier data from the *Torpedo* AChR, in both the steepness of the conductance-charge relation and in the net charge at which the conductance is half-maximal. Pappone and Barchfeld (1990) measured a 20% conductance reduction after extracellular trimethyloxonium treatment of AChRs in BC3H-1 cells. A +1 charge change in the extracellular ring would be sufficient to cause this reduction, if their result can be compared directly with our Fig. 4. A single trimethyloxonium treatment does not always modify all exposed acid groups (MacKinnon and Miller, 1989); it was not reported whether the AChRs were fully reacted. The 47% conductance reduction reported from tri-

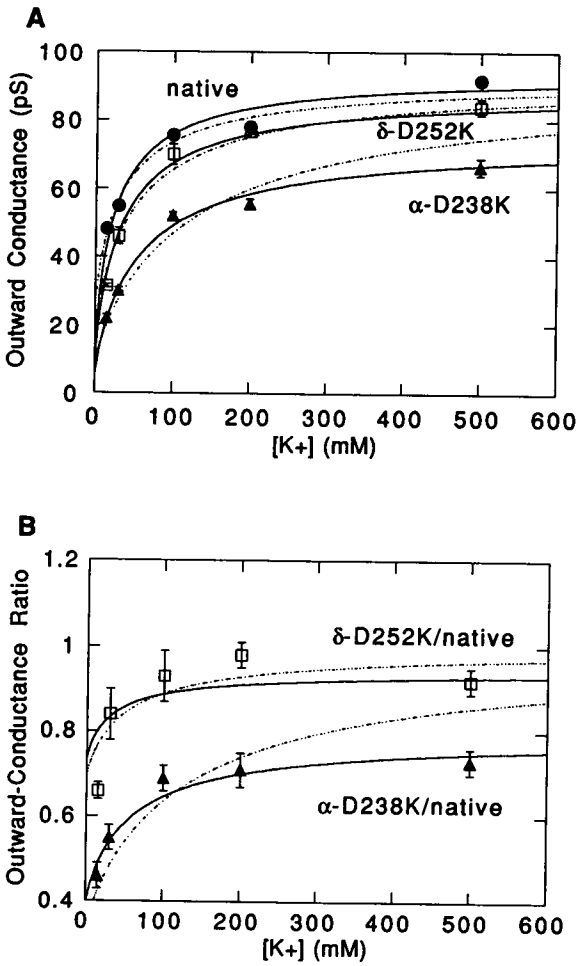

FIGURE 6 (*A*) Outward conductance of native AChR (*circles*) and cytoplasmic-ring mutants δ-D252K (*squares*) and α-D238K (*triangles*), plotted against $[K^+]$. (*B*) Mutant/native outward-conductance ratios versus $[K^+]$. The data in both figures are fit using the simple electrostatic model of Eqs. 3 and 4 (*dashed lines*) and the concentration-saturation model of Eq. 8 (*solid lines*).

methyloxonium treatment of frog muscle AChRs (Adams, 1983) may indicate that more residues were modified in those experiments.

We found that the changes in conductance produced by extracellular-ring mutations are essentially independent of ionic strength. This is consistent with previous results on chemical modification of the AChR from the extracellular side (Pappone and Barchfeld, 1990). The mutation δ-K276E raises (and the mutation α-E262Q lowers) the inward conductance by a constant factor over a range of $[K^+]$ from 15 to 500 mM. In contrast, increasing $[Mg^{2+}]$ from 0 to 1 mM does attenuate the effect of the mutation δ-K276E.

The effects of the cytoplasmic-ring mutations δ-D252K and α-D238K become more pronounced as the ionic strength is lowered below 100 mM, as expected for an electrostatic mechanism. The effects are not completely attenuated at high ionic strength, however.

The ionic-strength independence of the extracellular-ring mutations cannot be explained by the simple electrostatic model of Eqs. 3 and 4. Even the cytoplasmic-ring mutations, which show some effect at low ionic strength, are still inconsistent with the simple model. These failures raise the question of what makes the AChR different from other channels, which have been successfully described by electrostatic models. One possible explanation is that the charge mutations could induce a global change in pore structure. Alternatively, we consider some modifications which might salvage the electrostatic model: first, there could be an upper limit on the ion concentration in the pore mouth; and second, the charge mutations could affect the ionic energy in the narrow region of the pore, rather than merely altering superficial ion concentrations.

Concentration saturation at the pore mouth

Suppose that there is an upper limit to the concentration of permeant ions at the pore mouth. For instance, cations bound to sites on the channel could partially occlude the pore, as in the model of Dani (1986); or ion-ion repulsion within the channel vestibule could limit the ion concentration. We postulate that fixed negative charges in the pore mouth form cation binding sites, and that a cation must bind to a site before it can enter the single-ion occupancy region. Then the concentration of cations C_s bound to a site has the form

$$C_s = S/(1 + K_s/C_0), \tag{6}$$

where S is the effective concentration of binding sites, K_s reflects the binding affinity of a cation to a site, and C_0 is from Eq. 2. We also modify the surface-charge density in Eq. 4 to account for neutralization of fixed charge by bound ions, with the same binding affinity K_s as in Eq. 6:

$$\sigma_s = \sigma/(1 + C_0/K_s). \tag{7}$$

We suppose that a negative charge mutation creates binding sites, and hence increases S. Substituting C_s for C in equation 1 gives

$$g = \frac{g_{max}}{1 + (K_m/S)[1 + (K_s/C)\exp(z_K\phi_0 F/RT)]}. \tag{8}$$

Equation 8 simplifies to the form of Eq. 3, with the new parameters

$$g'_{max} = g_{max}/(1 + K_m/S) \tag{9a}$$

$$K'_m = K_s/(1 + S/K_m). \tag{9b}$$

In this model a positive charge mutation in either mouth of the channel decreases the apparent maximum conductance g'_{max} by decreasing the concentration of binding sites S relative to the intrinsic K_m, the ion concentration which would produce half-maximal conductance if there were no binding sites in the vestibule; the reverse holds for a negative charge mutation. The apparent binding affinity is

$$K_{app} = K'_m \exp(z_K\phi_0 F/RT). \tag{10}$$

A positive charge mutation can weaken the apparent affinity in two ways: it can raise K'_m by decreasing S/K_m, and it can make the surface potential ϕ_0 more positive. The apparent affinity K_{app} can be determined from the conductance-concentration relation, as the concentration producing half-maximal conductance; the mutant value of K_{app} also equals the concentration at which the mutant/native conductance ratio is midway between its high and low-concentration limits.

We fit the inward and outward conductance-concentration relations separately; for simplicity we use a common g_{max}, σ, and K_s for native and mutant channels, forcing S/K_m to account for the effects of the mutations (Table 6). The fitted conductances and conductance ratios are shown in Figs. 5 and 6 (*solid curves*). These parameter values are intended to illustrate the model; they are not uniquely determined by the data. The fits replicate the changes in maximum conductance and differences in apparent binding affinity between extracellular and cytoplasmic-ring mutants, although they do not fit the data precisely. Consistent with our expectation, S/K_m is larger for more negative mutants and smaller for more positive mutants. The inward and outward K'_m values (calculated from Eq. 9b and Table 6) decrease by roughly twofold for each decrease of four positive charges in the

TABLE 6 Best-fit parameters of concentration-saturation model

Parameter	Inward	Outward
g_{max} (pS)	224	111
σ (e/nm^2)	−0.04	−0.02
K_s (mM)	38	183
S/K_m	1.1 (Δz=−2)	5.7 (Δz=0)
	0.8 (Δz=0)	4.0 (Δz=2)
	0.3 (Δz=2)	2.1 (Δz=4)

Fits of conductance-concentration data. Parameters are from Eqs. 4, 7, and 8. The native AChR and each mutant (identified by Δz) has its own S/K_m. The data can be fit almost as well using a common K_s for inward and outward conduction.

appropriate ring. Thus similar mechanisms could control the ionic-strength dependence of extracellular and cytoplasmic-ring mutations, despite their apparent difference.

Electrostatic effect on ionic-energy barriers

Another possibility is that the charge mutations alter the ionic-energy profile in the narrow part of the pore, rather than changing only the local permeant-ion concentration in the pore mouth, as assumed in the model of Eq. 3 (although the local-concentration model can be treated formally as a change in the height of the energy barrier to ion entry). However, if the mutations act by an electrostatic mechanism, there are constraints on how they can affect the inward and outward maximum conductances, since the maximum conductance reflects the difference between peaks and wells in the ionic-energy profile. The extracellular ring is thought to be near the extracellular pore mouth, far from the selective region of the pore. Then assuming that the potential produced by a mutated charge decays monotonically with distance from the charge along the pore axis, a negative charge mutation in the extracellular pore mouth should tilt the ionic-energy profile toward the extracellular side (Fig. 7 *A*), increasing the outward maximum conductance and decreasing the inward maximum conductance. This constraint applies only to the maximum conductance; at low permeant-ion concentration the mutation can also increase the inward conductance by increasing the local ion concentration in the extracellular pore mouth (MacKinnon et al., 1989). In most channels electrostatic effects are attenuated at high ion concentrations, so the predicted asymmetry in charge effects on inward and outward maximum conductances has not been previously studied. All the mutations we have examined have similar effects on inward and outward maximum conductances, either increasing both or decreasing both. This suggests that the major effect of the ring charge mutations is in the middle of the ionic-energy profile, rather than at one end. This appears to be inconsistent with the supposed location of the extracellular ring, far from the major energy barriers.

However, this apparent inconsistency could reflect the inadequacy of the Gouy-Chapman formalism for describing the potential inside an ion channel. The electric field produced by a charge near a dielectric interface depends on the shape of the interface (Zauhar and Morgan, 1985). A continuum-dielectric model of the enzyme superoxide dismutase, accounting for electrolyte screening and the detailed shape of the enzyme, indicates that the potential field produced by a charge is focussed toward the low-dielectric, electrolyte-inaccessible protein interior (Klapper et al., 1986). A similar calculation for the AChR, applying the program DelPhi (Gilson et al., 1988) to a simplified version of the AChR-membrane structure (based on Toyoshima and Unwin, 1988), indicates that focussing of the potential might also occur in the AChR; the calculated potential produced by a charge located away from the pore axis (for instance, lining a wide vestibule, or on the exterior surface of the protein) is

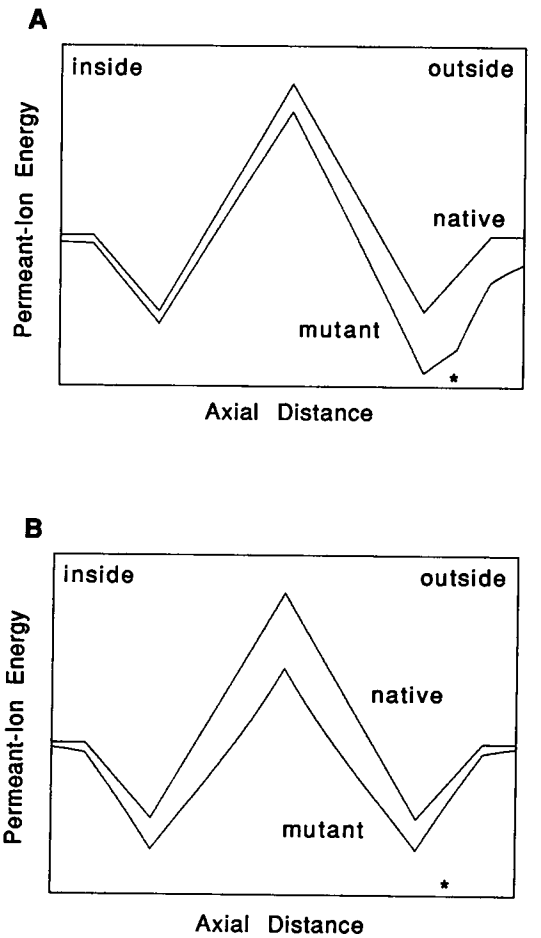

FIGURE 7 Schematic permeant-ion energy profiles for native AChR and a negatively charged extracellular-ring mutant. The position of the mutated charge, indicated by a star, is the same in *A* and *B*. The number of energy peaks and wells drawn is arbitrary. (*A*) If the potential produced by the mutated charge decays monotonically with axial distance from the charge, then the energy profile tilts to the right. (*B*) If the potential produced by the mutated charge is focussed toward the center of the membrane, then the energy peak is lowered more than either of the energy wells.

focussed toward the center of the membrane (G. Yellen, unpublished). In this way a negative charge mutation in the extracellular ring could lower a central ionic-energy peak more than the surrounding energy wells (Fig. 7 *B*), and hence increase both inward and outward maximum conductances, consistent with observation. These calculations also suggest another possible component of the unusual ionic-strength dependence of the conductance ratios: the calculated potential is relatively insensitive to electrolyte screening, even if the vestibules are completely accessible to electrolyte. Such effects of channel geometry could also explain the results of Konno et al. (1991): their AChR permeation model requires that a positive charge mutation in the extracellular ring raise a central ionic-energy barrier more than a nearer energy well.

Structural change

A third possibility is that a charge mutation induces a global change in the channel structure; for instance, it could change

the diameter of the narrow, selective region of the pore. This could alter the maximum conductance, perhaps with an unusual ionic-strength dependence. Charge-neutral mutations in the AChR at a residue corresponding to α-Thr244 are hypothesized to act through localized changes in pore diameter; the mutant/native conductance ratios differ for ions as close in diameter as K^+ (2.66 Å) and Rb^+ (2.96 Å) (Villarroel and Sakmann, 1992). Thus we expect that ions with such different dimensions as DMA^+ (3.8 × 4.2 × 6.1 Å (Sanchez et al., 1986)) and K^+ would reveal a change in pore diameter even more clearly, with the mutations affecting the conductance of the larger ion DMA^+ more than K^+ conductance. The relations between inward conductance and extracellular-ring charge (Fig. 4) show no conspicuous difference between DMA^+ and K^+, except for a uniform reduction in DMA^+ conductance relative to K^+ conductance. While our results do not indicate a global change in pore diameter, we cannot rule out some other sort of structural change.

Alternatives

It is possible that the saturation of conductance with increasingly negative extracellular-ring charge (Fig. 4) is due in part to incomplete ionization of the acidic side chains in the ring; such a mechanism has been suggested by Dani and Eisenman (1987). For an acidic side chain to be ionized less than 90% of the time requires (pH − pK) < 1; at first this appears unlikely given the experimental conditions (pH = 7.5 and pK ≈ 4.5). However, the local H^+ concentration at the surface of a negatively charged membrane is elevated relative to its bulk concentration; the surface pH at moderate ionic strength can be lowered by 1.6 units (Menestrina et al., 1989; van der Goot et al., 1991). (At 100 mM ionic strength a Gouy-Chapman surface-charge density of −0.7 e/nm^2 would lower the local pH by 1.6 units.) Although the potential produced by lipid charges has not been shown to affect AChR conductance, charges on the channel protein could have a similar effect on the local pH. It is also possible that the pK of an acidic side chain is higher than its intrinsic value; deviations in pK of up to 1.7 units have been observed for ionizable residues in water-soluble proteins (Matthew, 1985). It has not been established whether electrostatic interactions alone are responsible for the pK shifts.

Our models have assumed that the major permeation barriers lie in a single-ion occupancy region. Streaming-potential measurements indicate that the narrow region of the AChR pore is too short to hold more than one ion at a time, supporting the use of such models (Dani, 1989). Multiple-ion occupancy models may nonetheless provide alternative explanations for our results; Konno et al. (1991) used a double-occupancy model to fit their results.

The use of a charged, impermeant open-channel blocker such as QX-222 (Charnet et al., 1990) may be useful to further test electrostatic models for the effects of extracellular charge mutations. Its association and dissociation rates can be measured directly, avoiding some of the uncertainties of interpreting permeant-ion transport rates. In addition, it blocks at sufficiently low concentrations that it would not have much effect on the ionic strength, and might avoid the concentration saturation in the vestibule discussed above.

We thank Dr. James B. Matthew for his comments, and Dr. James D. Lear for countless discussions.

This research was supported by the Howard Hughes Medical Institute, by National Institutes of Health Grant K08 HL02421-02 (G. T.), and by Grant 3243 of the Council for Tobacco Research (G. Y.). Dr. Tomaselli is an Eli Lilly Clinician-Scientist of the Johns Hopkins School of Medicine.

REFERENCES

Adams, D. J. 1983. Chemical modification of endplate channels in frog skeletal muscle. *J. Physiol. (Lond.)*. 343:29P–30P. (Abstr.)

Apell, H.-J., E. Bamberg, H. Alpes, and P. Läuger. 1977. Formation of ion channels by a negatively charged analog of gramicidin A. *J. Membr. Biol.* 31:171–188.

Apell, H.-J., E. Bamberg, and P. Läuger. 1979. Effects of surface charge on the conductance of the gramicidin channel. *Biochim. Biophys. Acta.* 552: 369–378.

Bell, J. E., and C. Miller. 1984. Effects of phospholipid surface charge on ion conduction in the K^+ channel of sarcoplasmic reticulum. *Biophys. J.* 45:279–287.

Boulter, J., W. Luyten, K. Evans, P. Mason, M. Ballivet, D. Goldman, S. Stengelin, G. Martin, S. Heinemann, and J. Patrick. 1985. Isolation of a clone coding for the α-subunit of a mouse acetylcholine receptor. *J. Neurosci.* 5:2545–2552.

Buonanno, A., J. Mudd, V. Shah, and J. P. Merlie. 1986. A universal oligonucleotide probe for acetylcholine receptor genes. Selection and sequencing of cDNA clones for the mouse muscle β subunit. *J. Biol. Chem.* 261:16451–16458.

Cecchi, X., O. Alvarez, and R. Latorre. 1981. A three-barrier model for the hemocyanin channel. *J. Gen. Physiol.* 78:657–681.

Charnet, P., C. Labarca, R. J. Leonard, N. J. Vogelaar, L. Czyzyk, A. Gouin, N. Davidson, and H. A. Lester. 1990. An open-channel blocker interacts with adjacent turns of α-helices in the nicotinic acetylcholine receptor. *Neuron.* 2:87–95.

Coronado, R., and H. Affolter. 1986. Insulation of the conduction pathway of muscle transverse tubule calcium channels from the surface charge of bilayer phospholipids. *J. Gen. Physiol.* 87:933–953.

Dani, J. A. 1986. Ion-channel entrances influence permeation. Net charge, size, shape, and binding considerations. *Biophys. J.* 49: 607–618.

Dani, J. A. 1989. Open channel structure and ion binding sites of the nicotinic acetylcholine receptor channel. *J. Neurosci.* 9:884–892.

Dani, J. A., and G. Eisenman. 1987. Monovalent and divalent cation permeation in acetylcholine receptor channels. Ion transport related to structure. *J. Gen. Physiol.* 89:959–983.

Gilson, M. K., K. A. Sharp, and B. H. Honig. 1988. Calculating the electrostatic potential of molecules in solution: method and error assessment. *J. Computational Chem.* 9:327–335.

Green, W. N., and O. S. Andersen. 1991. Surface charges and ion channel function. *Annu. Rev. Physiol.* 53:341–359.

Imoto, K., C. Busch, B. Sakmann, M. Mishina, T. Konno, J. Nakai, H. Bujo, Y. Mori, K. Fukuda, and S. Numa. 1988. Rings of negatively charged amino acids determine the acetylcholine receptor channel conductance. *Nature (Lond.).* 335:645–648.

Imoto, K., C. Methfessel, B. Sakmann, M. Mishina, Y. Mori, T. Konno, K. Fukuda, M. Kurasaki, H. Bujo, Y. Fujita, and S. Numa. 1986. Location of a δ-subunit region determining ion transport through the acetylcholine receptor channel. *Nature (Lond.).* 324:670–674.

Klapper, I., R. Hagstrom, R. Fine, K. Sharp, and B. Honig. 1986. Focusing of electric fields in the active site of Cu-Zn superoxide dismutase: effects of ionic strength and amino-acid modification. *Proteins Struct. Funct. Genet.* 1:47–59.

Konno, T., C. Busch, E. von Kitzing, K. Imoto, F. Wang, J. Nakai, M. Mishina, S. Numa, and B. Sakmann. 1991. Rings of anionic amino acids as structural determinants of ion selectivity in the acetylcholine receptor channel. *Proc. R. Soc. Lond. B Biol. Sci.* 244:69–79.

LaPolla, R. J., K. M. Mayne, and N. Davidson. 1984. Isolation and characterization of a cDNA clone for the complete protein coding region of the δ subunit of the mouse acetylcholine receptor. *Proc. Natl. Acad. Sci. USA.* 81:7970–7974.

Läuger, P. 1973. Ion transport through pores: a rate-theory analysis. *Biochim. Biophys. Acta.* 311:423–441.

Lewis, C. A., and C. F. Stevens. 1979. Mechanism of ion permeation through channels in a postsynaptic membrane. *In* Membrane Transport Processes, vol. 3. C. F. Stevens and R. W. Tsien, editors. Raven Press, New York. 133–151.

MacKinnon, R., R. Latorre, and C. Miller. 1989. Role of surface electrostatics in the operation of a high-conductance Ca^{2+}-activated K^+ channel. *Biochemistry.* 28:8092–8099.

MacKinnon, R., and C. Miller. 1989. Functional modification of a Ca^{2+}-activated K^+ channel by trimethyloxonium. *Biochemistry.* 28:8087–8092.

Matthew, J. B. 1985. Electrostatic effects in proteins. *Annu. Rev. Biophysics Biophys. Chem.* 14:387–417.

McLaughlin, S. 1989. The electrostatic properties of membranes. *Annu. Rev. Biophysics Biophys. Chem.* 18:113–136.

McLaughlin, S. G. A., G. Szabo, and G. Eisenman. 1971. Divalent ions and the surface potential of charged phospholipid membranes. *J. Gen. Physiol.* 58:667–687.

Menestrina, G., S. Forti, and F. Gambale. 1989. Interaction of tetanus toxin with lipid vesicles. Effects of pH, surface charge, and transmembrane potential on the kinetics of channel formation. *Biophys. J.* 55:393–405.

Moczydlowski, E., O. Alvarez, C. Vergara, and R. Latorre. 1985. Effect of phospholipid surface charge on the conductance and gating of a Ca^{2+}-activated K^+ channel in planar lipid bilayers. *J. Membr. Biol.* 83:273–282.

Pappone, P. A., and G. L. Barchfeld. 1990. Modifications of single acetylcholine-activated channels in BC3H-1 cells. Effects of trimethyloxonium and pH. *J. Gen. Physiol.* 96:1–22.

Reinhardt, R., K. Janko, and E. Bamberg. 1986. Single channel conductance changes of the desethanolamine-gramicidin through pH variations. *In* Electrical Double Layers in Biology. M. Blank, editor. Plenum Press, New York. 91–102.

Roeske, R. W., T. P. Hrinyo-Pavlina, R. S. Pottorf, T. Bridal, X.-Z. Jin, and D. Busath. 1989. Synthesis and channel properties of [Tau^{16}]gramicidin A. *Biochim. Biophys. Acta.* 982:223–227.

Sanchez, J. A., J. A. Dani, D. Siemen, and B. Hille. 1986. Slow permeation of organic cations in acetylcholine receptor channels. *J. Gen. Physiol.* 87:985–1001.

Sigworth, F. J., and B. C. Spalding. 1980. Chemical modification reduces the conductance of sodium channels in nerve. *Nature (Lond.).* 283:293–295.

Tomaselli, G. F., J. T. McLaughlin, M. E. Jurman, E. Hawrot, and G. Yellen. 1991. Mutations affecting agonist sensitivity of the nicotinic acetylcholine receptor. *Biophys. J.* 60:721–727.

Toyoshima, C., and N. Unwin. 1988. Ion channel of acetylcholine receptor reconstructed from images of postsynaptic membranes. *Nature (Lond.).* 336:247–250.

Van der Goot, F. G., J. M. González-Mañas, J. H. Lakey, and F. Pattus. 1991. A 'molten-globule' membrane-insertion intermediate of the pore-forming domain of colicin A. *Nature (Lond.).* 354:408–410.

Villarroel, A., and B. Sakmann. 1992. Threonine in the selectivity filter of the acetylcholine receptor channel. *Biophys. J.* 62:196–208.

Worley, J. F., III, R. J. French, and B. K. Krueger. 1986. Trimethyloxonium modification of single batrachotoxin-activated sodium channels in planar bilayers. *J. Gen. Physiol.* 87:327–349.

Yu, L., R. J. LaPolla, and N. Davidson. 1986. Mouse muscle acetylcholine receptor γ subunit: cDNA sequence and gene expression. *Nucleic Acids Research.* 14:3539–3555.

Zauhar, R. J., and R. S. Morgan. 1985. A new method for computing the macromolecular electric potential. *J. Mol. Biol.* 186:815–820.